International Journal of Integrated Engineering – Special Issue on Electrical Electronic Engineering
Vol. 9 No. 4 (2017) p. 64-75

Artificial Neural Network and Wavelet Features Extraction Applications in Nitrate and Sulphate Water Contamination Estimation

Aizat Azmi[1], Khairell Khazin Khaman[1], Sallehuddin Ibrahim[1], Mohd Taufiq Md Khairi[1], Mahdi Faramarzi[1], Ruzairi Abdul Rahim[3], Mohd Amri Md Yunus[2*]

[1]Protom-i Research Group, Innovative Engineering Alliance,
[2]Micro-Nano Systems Engineering Research Group, Frontier material,
Faculty of Electrical Engineering,
Universiti Teknologi Malaysia, 81310, Skudai, Johor, Malaysia.
[3]Universiti Tun Hussein Onn Malaysia, 86400 Parit Raja, Johor.

Abstract: This work expounds the review of non-destructive evaluation using near-field sensors and its application in environmental monitoring. Star array configuration of planar electromagnetic sensor is explained in this work for nitrate and sulphate detection in water. The experimental results show that the star array planar electromagnetic sensor was able to detect nitrate and sulphate at different concentrations. Artificial Neural Networks (ANN) is used to classify different levels of nitrate and sulphate contaminations in water sources. The star array planar electromagnetic sensors were subjected to different water samples contaminated by nitrate and sulphate. Classification using Wavelet Transform (WT) was applied to extract the output signals features. These features were fed to ANN consequently, for the classification of different levels of nitrate and sulphate concentration in water. The model is capable of distinguishing the concentration level in the presence of other types of contamination with a root mean square error (RMSE) of 0.0132 or 98.68% accuracy.

Keywords: Artificial neural network; wavelet transform; planar electromagnetic sensors array; nitrate contamination; sulphate contamination.

1. Introduction

Non-destructive testing provides reliable information of the material under investigation to be perceived as safe, reliable, and usable [1]. Many of the interdisciplinary field of non-destructive testing, non-destructive testing and evaluation based on electromagnetic approaches are gaining worldwide attention since it was introduced due to simplicity, fast response, convenience, and low cost. A particular electromagnetic approach of interest is the non-destructive testing or inspections based on the inductive and capacitive or electromagnetic effects. Such devices or sensors can be seen in the industrial areas [2], agriculture [3], and engineering/scientific application (e.g. land mine detection) [4], health and food monitoring [5], manufacturing [6, 7], automation [8], structure inspection [9] etc.

The sensing or/and exciting elements of a planar electromagnetic device usually have flatten structures and separated by substrates e.g FR4, alumina etc. Several examples of planar electromagnetic systems are discussed in this section. Inductive planar electromagnetic devices have been reported in [10-19] and extension used as sensors for testing (nondestructive testing) the integrity of materials (conductive and magnetic material) in [20-29]. Inductive planar sensors are also used as proximity and displacement sensors [17, 30]. A method for inspecting the integrity of different coins, which can successfully discern different types of coins using meander planar sensors has been demonstrated [31]. Capacitive planar electromagnetic sensors or commonly known as coplanar interdigital sensors have been used for many applications, some of the examples are moisture measurement in pulp [32], monitoring the impedance change caused by the growth of immobilized bacteria [33], human health confirmation based on the content of water in human skin [34], humidity sensors [35], food inspection for human safety, non-invasive monitoring of industrial and medical applications [36-39], and estimation of material dielectric properties such as food and saxophone reeds [40-44]. A sensing system based on the interdigital sensor has been developed for determining the looseness in sheep skins. A good correlation was observed between the sensor output voltage and looseness values for both before and after tanning process. The formula for calculating of looseness was developed, and on comparison with the actual looseness values, they were quite proximate [45].

Therefore, the application and structure of mender and interdigital sensor will be further elaborate in the later section. This paper is divided into 5 sections. Section 1 presents the basic concept of electromagnetic approach for non-destructive testing. The basic structure and application

*Corresponding author: amri@fke.utm.my

penerbit.uthm.edu.my/ojs/index.php/ijie

of planar electromagnetic sensor are discussed. Meanwhile, Section 2 highlights the drawbacks of previous development of electromagnetic sensor as well as its applications. Section 3 discusses the architecture and measurement concept of planar electromagnetic sensor for nitrate and sulphate detection. Besides, section 4 discusses on Artificial Neural Network (ANN). The classification process of contaminants is done through experimental and detail explanation is also discussed. Lastly, section 5 concludes the feasibility of ANN to estimate nitrate and sulphate in water.

2. Application of Non-Destructive Sensor for Environmental Monitoring

For the past ten years, the research of environmental monitoring based on planar meander and interdigital elements has followed several avenues. The early work (since 2001) involved a serially closed circuit inductor-capacitor (LC) element, (Titanium Dioxide) TiO2 coating, and flexible parallel plate capacitor which forms a passive sensor. The sensor operates on wireless and remote query basis has been applied for environmental parameters monitoring based on complex permittivity of a surrounding medium, temperature monitoring, and pressure [46]. Later on, this work evolved into other application such as bacteria growth monitoring [47, 48], monitoring of electrical properties of biological cell solutions [49], quantifying packaged food quality [50], and real-time monitoring of water content in civil engineering materials [51, 52]. Despite of offering a good performance, this system is quite complex, considering the material properties estimation was achieved from impedance spectrum of the sensor measured using a remotely located antenna. The material properties (e.g. complex permittivity) are calculated from the impedance spectrum at the resonant frequency with the inductance and capacitance of the sensor values based on calculation of an analytical model. Moreover, looking at the current technologies, the potential of this system to be a portable or home appliance is hindered, as it requires either an expensive impedance analyzer or lock-in amplifier.

Having a resemblance sensor design, Stanley et al. [53] and Woodard [54] employed open-circuited self-resonating planar spiralling pattern of electrically conductance material coated with active material. The results reflected that the sensors are suitable to be used in harsh condition. Nevertheless, the material used to make the sensor i.e. Silicon Nitride (Si3N4) is relatively expensive and only affordable by programs funded for space exploration. Dickey et al. [55] and Oommon et al. [56] have investigated the effect of different size of pore and uniformity of the substrate (Metal Oxide) which was made as a platform base for interdigital sensor on the sensitivity and accuracy of NH3 and relative humidity. Metal Oxide materials (SnO2, Al2O3, and TiO2) are relatively low cost and well-known for their manipulatable structure for gas-sensing enhancement. However, the fabrication of the sensor is laborious that requires an access to expensive facilities and considerably skilled personnel.

Several researchers [57, 58] have address the application of Inductor and Capacitor (LC) wireless sensor with Elecrolyte-Nitrate-Oxide-Silicon (ENOS) structure as an electrochemical potential-to-capacitance transductor fabricated using CMOS technology for pH measurement of liquid material such as water. These studies have made improvement of shorter response time and linear response. The main drawback is the operating frequency had to be adjusted to a proper value to minimize the unwanted response of the sensor to the sample (material under test) conductivity. In this study, our attention and interest have been drawn into to develop an electromagnetic sensor consisting both inductive and capacitive element which can be integrated as a low cost, convenient, and suitable for in-situ measurement system for water quality monitoring which will contribute to environmental monitoring. Detection of pollutants especially in drinking water is crucial in order to avoid negative impact on human health.

3. Planar Electromagnetic Sensor as a Near Field Sensor

Every material has different electrical properties. By taking advantage of this fact, planar electromagnetic sensors have been widely utilized for inspection of near-to-the-surface properties such as dielectric, permeability and permittivity [67, 68], food safety and fat content in milk and bacterial content [36-39] are common applications that use planar electromagnetic sensors as a detection device.

3.1 Planar meander and interdigital sensors

The application of meander type sensor is widely found in dairy product industry [69] and PCB board production [70]. The meander type sensor consists of an exciting circuit and a sensing circuit that is placed close to each other as illustrated in Fig. 1 [71, 72]. A high frequency alternating current is supplied to the exciting current to induce eddy current on the circuit.

Meanwhile, the sensing circuit absorbs or picks up the variation of magnetic field. This sensing circuit compliments the Faraday's law which stated that a voltage will be generated when placed in a moving electromagnetic field [73].

There is an extensive research involving areas such as photosensitive detectors, surface acoustic waves, humidity

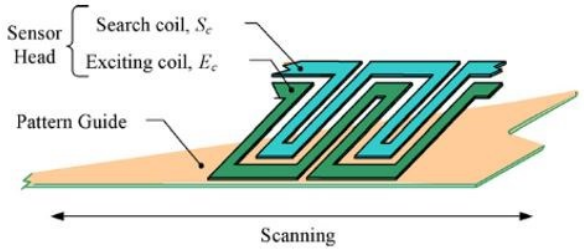

Fig. 1 A basic meander type sensor [11]

sensors and sensors for chemicals and gasses which used the interdigital electrode [36]. As reported in [74-76], the estimation of dielectric properties of leather, seafood and platelet using interdigital sensors to determine its characteristics such as quality, contaminant and concentration was successful. Fig. 2 shows the interdigital type sensor. The operational principle of interdigital sensor is similar to the parallel plate capacitor where one side is connected to the AC voltage source and another side is grounded. The interlocking arrays of positive and negative electrodes structure is applied to gain enough capacitive value to provide sufficient electric field in order to penetrate the medium under test [77].

The main advantage of planar electromagnetic sensor is the fabrication process can be completed on a printed-on circuit board (PCB) thus incurred minimum fabrication cost. Fig. 3 illustrates the planar electromagnetic sensor that has been fabricated on PCB with two layers [78].

3.2 Planar Electromagnetic Sensor for Nitrate and Sulphate Detection

Planar electromagnetic sensor could be developed by combining the meander and interdigital type sensor. The combination of these two sensors would produce an electromagnetic field where the magnetic field is produced by the meander type sensor and the electric field is being generated by the interdigital type sensor. As reported in [29], the combination of the meander and interdigital type give the best sensitivity.

The meander structure in an electromagnetic sensor consists of five loops with an overall dimension of 20 × 20 mm. The gap between each loop and the width of each loop is set to be 0.5mm. On the other hand, the interdigital structure in an electromagnetic sensor consists of five positive electrodes and four negative electrodes. The width of a positive electrode and a negative electrode is 0.5 mm and 1.0 mm respectively. Fig. 4 illustrates the meander and interdigital type sensor that is connected in series to form an electromagnetic sensor.

The wider negative electrode of interdigital type sensor is recommended by Yunus et al. [79, 80] for a better response. Apart from that, a wider and bigger ground backplane with a dimension of 10 mm × 8 mm as shown by the red color in Fig. 4(b) is needed to reduce interference. The output strength of an interdigital sensor could be increased by manipulating the distance between each electrode [81]. In order to operate the sensor, a source of alternating 10 Volt peak to peak sinusoidal waveform is supplied from a function generator. The magnetic field generated by meander type sensor is combined with the electric field generated by interdigital type sensor to form an electromagnetic field. This electromagnetic field interacted with the medium or material under test. The dielectric properties of the material will alter the electromagnetic field of the sensor and consequently, change the impedance of the sensor that is being measured across the terminal. However, the previous model of planar electromagnetic sensor could only take one reading per time due to the single structure of the sensor [79]. The data

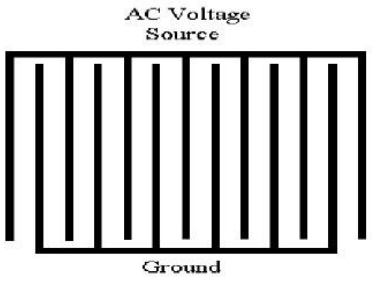

Fig. 2 The interdigital type sensor [17]

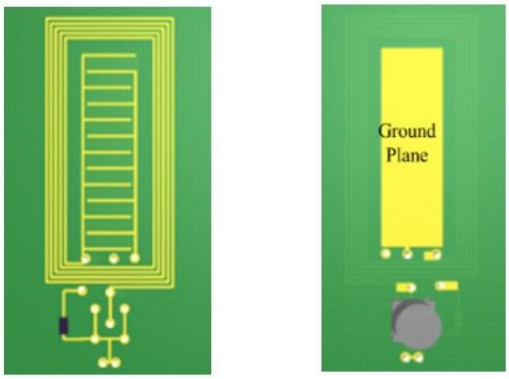

(a) Top layers (b) bottom layers

Fig. 3 planar electromagnetic sensor illustration [78]

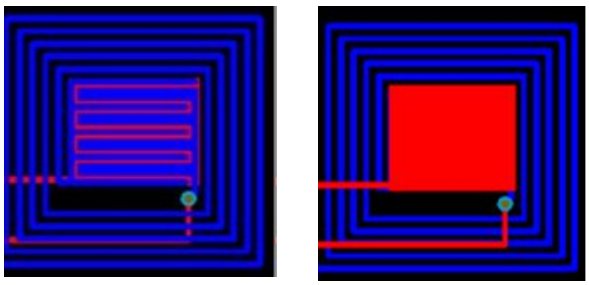

(a) Top view *(b) Bottom view*

Fig. 4 The planar electromagnetic sensor design [29]

collection need to be taken several times before being analysed. As such the single detection method consumed a lot of time before analysis could be done. Hence, the planar electromagnetic sensors array is introduced.

This paper used the star array planar electromagnetic sensors as developed in [82, 83], for nitrate and sulphate detection in water. The design for the star array configuration is illustrated in Fig. 5, where the difference between each array is the placement of sensors S_1, S_2 and S_3. Based on Fig. 5, sensor S_2 is located 10mm away from sensor S_1 before being rotated at 45° clockwise as this configuration provides higher sensitivity. On the other hand, sensor S_3 is also located 10 mm away from sensor S_1 and is rotated at 45° anti clockwise. Fig. 5(a) shows the top configuration that is filled with blue color. At the same time, this blue color indicated the series connection of meander and interdigital type sensor. All of these three

sensors are connected to the same function generator at the same node. Fig. 5 (b) shows the bottom view where the connection is colored with red. This red color represents the ground backplane structure of a star array configuration.

An electrical equivalent circuit of the star sensor array is shown in Fig. 6. According to Fig. 6, the sensor is connected to a function generator where R_g is the output resistance with a nominal value of 50 Ω. R_1 denotes the series surface mount resistor connected to sensor 1 (S_1). Hence, current I_{3-1} can be calculated from

$$I_{3-1} = V_{3-1} / R_1 \quad (1)$$

where I_{3-1} and V_{3-1} are the rms value of current through the sensor and voltage across R_1 respectively. The absolute total impedance for sensor S1, Z_1 is given by

$$Z_1 = V_1 / I_{3-1} \quad (2)$$

$$Z_1 = V_1 \angle \theta_1 / I_{3-1} \angle 0^\circ \quad (3)$$

The same method of calculation can be used to calculate the impedance for both sensors S_2 and S_3 by using Equations (2) to (3).

In [83] the measurement for nitrate and sulphate is then carried out for data acquisition. The experimental setup is shown in Fig. 7 where the setup has a frequency waveform generator which generated standard sinusoidal waveform with 10 Volts peak-to-peak value and was set as the input signal for the sensors. A retort stand was used to hold the star sensor array. The star sensor array was partially immersed into the water sample. A signal oscilloscope was interfaced to a PC where the output signals and the sensor's impedance was calculated using LabVIEW software. The measurements were done at frequency range between 1 kHz and 10 MHz. Before the experiment, Wattyl Killrust Incralac is sprayed to the sensors in order to form an acrylic resin-based protective coating. The effect of the samples on the sensor's impedance was recorded. The measurement data is then analyzed by the artificial neural network (ANN) for contaminants classification.

4. Planar Electromagnetic Sensor For Nitrate & Sulphate Detections using ANN

In this section, how ANN can be used to classify nitrate and sulphate contaminations using star array configuration is discussed in details. A complex, nonlinear relationship between inputs and outputs with many adjustable parameters such as weights and biases was demonstrated by ANN. The ANN needs to undergo three different stages known as training, validation and testing. During the training session, the adjustable parameters that are used could be optimized. For example, in the situation in which the input is unknown or "unseen" but, if the data set is sufficiently provided and meet the training procedure of ANN, the output still can be recognized by the ANN [84].

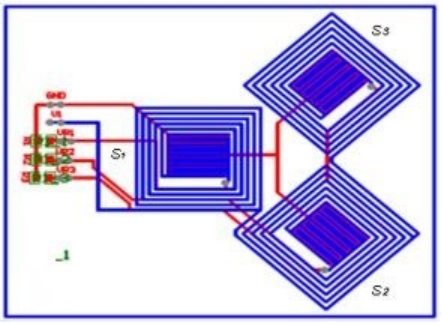

(a) Top view

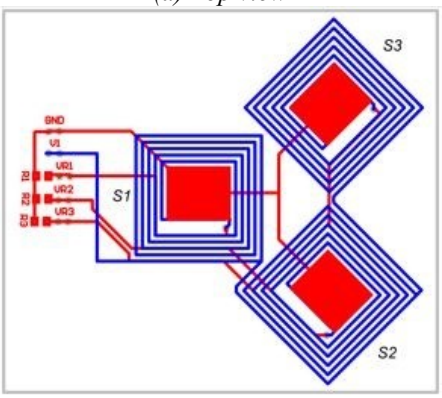

(b) Bottom view

Fig. 5 Star array configuration of planar electromagnetic sensor

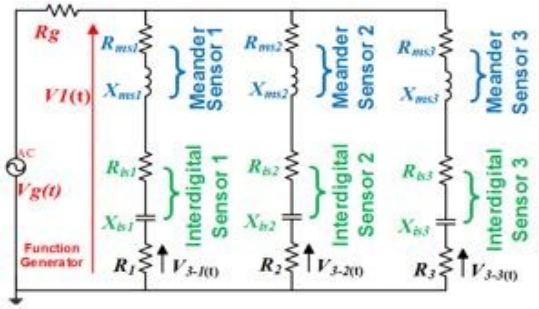

Fig. 6 Equivalent circuit for star sensor array

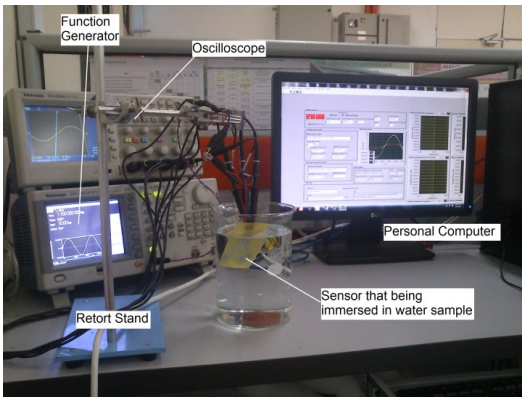

Fig. 7 Experimental setup for determination of nitrate and sulphate

Basically, the traditional ANN comprises of three layers: input data where the data is introduced into the system, the hidden layer (layers) and the output layer [85]. Every single layer consists of many different elements called neurons. A neuron can be specified as a nonlinear function and has a parameterized boundary value. Besides, each neuron has its own activation function that connected each other with a variable weighting value.

Different types of neural network can be varied by the neural interconnection (architecture), methods of adjusting the weight and the different activation functions. The neural network can be categorized as supervised neural network and unsupervised neural network. Feed forward neural network (FFNN) is a short term for supervised neural network, which consists of an input layer, a hidden layer(s) and output layer. Multilayer perceptron (MLP) is another branch of FFNN in which the neuron in each layer is only connected to the adjacent layer. Each layer contains a predetermined number of neuron and activation function.

4.1 Hidden Layers and Nodes of ANN

The number of hidden layers and the number of neurons in each layer is determined by the degree of difficulty of a problem and can be obtained by a trial and error method. The error of the network would increase if the number of neurons is not enough. Usually, the number of neurons increased in a highly non-linear problem and decreased in a simple problem. According to Gybelco [86], finding the number of neurons is still a challenge even though a three layer perceptron involved an arbitrary nonlinear, continuous, and multidimensional function. Selection of appropriate neurons number is a must where the large number of neuron caused over fitting of the neural network. On the other hand, inadequate neurons number caused the network function to be impaired. Hence, a trial and error method is used in this case to find an appropriate neurons number for three layers MLP neural network.

4.2 Weight Initialization for ANN

Weight is one of the crucial part in ANN. The wrong selection of weight and biases could lead to a local minima problem. Therefore, these two parameters need to be initialized first before being trained by the Back Propogation (BP) algorithm. These values are normally initialized by selecting a random non-zero value between interval of [-1, 1] and yet, it still cannot guarantee that these values are the local minima of the network. In order to overcome this problem, it has to start again from a selection of different values and go through the similar training process to reach the global minima.

4.3 ANN Back Propagation Learning Algorithm

The network is ready for training after the weight and biases of MLP neural network are initialized. The most common and popular algorithm for MLP training is Back Propagation (BP). BP algorithm was introduced by Rumelhert *et. al* in 1986 [82]. In the BP training process, a set of data vectors known as inputs and target outputs is required. The main objective of BP is to reduce the backward propagated error. During the BP training, the neurons already organized themselves to send the signals forward and then the last output of the last layer is compared with the real output data sets. After that, the errors are propagated back to the input data in the network. This process continued until the stopping criteria is satisfied.

Conventional BP used a gradient descent algorithm which could gradually reduce the Mean Square Error (MSE) of output data during the epochs. The MSE for network can be shown as:

$$E = \frac{1}{N}\Sigma_{i=1}^{N}(T_i - O_i)^2 \qquad (4)$$

where, O is network output, T is target output and N is the number of samples.

The network weights and biases is updated with a simple gradient descent algorithm in the direction where the performance function decrease rapidly by adding the negative of the gradient to the current parameters as shown:

$$w_{t+1} = w_t - \alpha g_t \qquad (5)$$

where, t is the time, α is the rate of learning, g is the gradient vector and w_t is the current weight matrix.

4.4 Stopping criteria

During the training session, the train set data is used to update the weights while the validation data set is applied to avoid over-fitting. The learning session is continued until the stopping criteria is achieved. The stopping criteria can be chosen either an exact number of iteration (epochs), an arbitrary level of low error (error level due to the problem dependent) or an epochs that increased the validation error.

4.5 Input Variables and data processing

The data set comprises of signals from different water contamination levels that is being measured by three planar electromagnetic sensors under different frequencies ranging from 1 kHz to 10 MHz. The large number of raw signals caused it to be unsuitable to feed neural networks. Hence, the dimension of these input signals for neural network must be reduced to an acceptable numbers where the procedures is known as feature extraction. Due to the non-stationary behaviour of these input signals, a Wavelet Transform (WT) can be used for decomposition and feature extraction.

4.5.1 Input Variables and data processing

A basis function called small wavelets with a limited duration is used by the Wavelet Transform (WT) to represent other functions based on the following formula:

$$F(a,b) = \frac{1}{\sqrt{a}} \int_{-\infty}^{\infty} \psi^*(\frac{t-b}{a}) f(t) dt \quad (6)$$

where, F is known as the Continuous Wavelet Transform (CWT) of $f(t)$ with scale a and translation b and ψ is called as the mother wavelet. The main position of the signal is determined by the translation factor while the scaled factor of wavelets allowed the signal with different scale value to be analysed. Equation (6) is an extended version of Wavelet. However, for a discrete signals, a Discrete Wavelet Transform (DWT) is needed for analysis and synthesis on the original signals.

In order to decompose the signals in different scales, the DWT used a series of low pass and high pass filters with different cut-off frequencies. These filters separated the original signal into two parts known as coarse approximation and detail information. Firstly, the original signal is passed through a high pass filter and a low pass filter. As a result, half of the samples were eliminated due to the output response of the filters that was down sampled by two. This procedure continued using the result of high pass filter until a pre-determined level is achieved. Fig. 8 illustrates the whole procedure for the two levels of signals decomposition.

4.5.2 Feature extraction

Feature extraction plays an important role in classification problems where this stage involved the dimension reduction. So far, there is no direct method that have been reported for finding the proper features. Besides, it should be done by trial and error method. Therefore, in this research, two features were extracted known as energy and mean. These two features are determined by the following formulas:

$$Energy(x) = \sum_{n=1}^{N} |x(n)|^2 \quad (7)$$

$$Mean(x) = \frac{1}{N} \sum_{n=1}^{N} x(n) \quad (8)$$

where, N is the number of samples and x is the sample. Hence, these features are used as an input for neural network.

4.6 Classes of Water Samples

The classes of water samples comprise of three groups of contamination which are Potassium Nitrate (KNO_3), Potassium Sulphate (K_2SO_4) and a combination of Potassium Nitrate and Potassium Sulphate (KNO_3 + K_2SO_4). These solutions are prepared at different concentration levels from 5 part per million to 115 part per million (ppm). From these three groups of contamination, each group comprises of different classes based on different amounts of concentration. In total, there are 19 classes altogether, in which there are 36 sets of samples in each class.

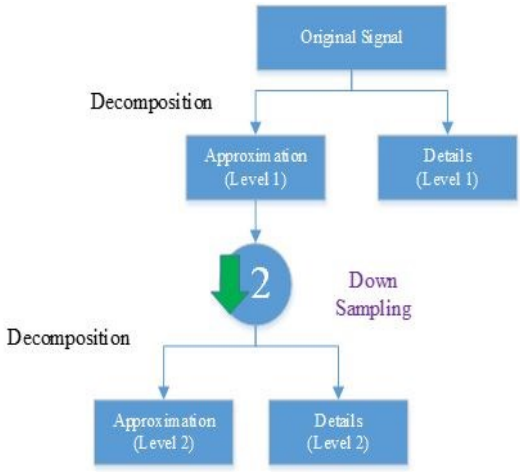

Fig. 8 Two levels of decomposition via Wavelet Transform

The advantage of planar electromagnetic sensors with the star array configuration is proved where only 12 measurements at a time is needed to obtain 36 sets of sample instead of 36 measurements. This advantage is due to the increase in the number of sensors in each measurement. Table 1 summarizes the different water contamination levels that represent the classes in each group for the reference sets.

4.7 Derivation of Impedance Sensitivity

The signals that are going to be feed or used by the ANN are based on the sensitivity of each sensor. The sensitivity is calculated based on the impedance of each sensor where the impedance is measured across the series resistor as governed by the following equation:

$$\%Z = \frac{(Z_{sample} - Z_{DistilledWater})}{Z_{DistilledWater}} \times 100\% \quad (9)$$

where, $\%Z$ is the impedance sensitivity, Z_{sample} is the impedance of the sensor when the sensor is immersed in the respective water sample, and $Z_{Distilled\ Water}$ is the impedance of the sensor in distilled water. The impedance sensitivity of each sensor have almost a similar magnitude at the respective frequency. Hence, it is not suitable to directly apply the signal from impedance sensitivity as it is difficult to differentiate each signal which has the same concentration of contamination type and level. Therefore, the normalized second derivative is applied to overcome this problem. In addition, the unwanted baseline level can be eliminated together based on the following equation:

$$\%Z'' = d^2(\%Z) / df^2 \quad (10)$$

where, $\%Z''$ is the normalized second derivative of impedance sensitivity of sensor and $\%Z$ is the impedance sensitivity of sensor. Figs. 9 and Fig.s 10 show the normalized second derivative of impedance sensitivity for three different classes of nitrate and sulphate, respectively.

4.8 Implementation of Wavelet Transform

There are different types of mother wavelets such as Haar, Daubichies, Coinflet and Symmlet that could be found in literatures. In this research, the Haar wavelet which is amongst the most popular wavelet is going to be used to decompose signals in 4 levels as illustrated in Figs. 11.

Figs. 11 (b) to (c) show that, the active parts of the decomposed signals are available at low frequency and high frequency for low level decomposition and high level decomposition, respectively. This shows a strong evidence that the details at each level of signals decomposition contain a different information extracted from the original signal.

4.9 Input Space for Neural Network

The main objective of water contamination classification is to demonstrate the effectiveness of energy and mean features for the normalized second derivative of *%Z''*. In order to accomplish this objective, the feature vectors in each class as shown in Table 2 are set as the input for the neural network.

Based on Table 1, there are 19 contamination classes based on potassium nitrate, KNO_3, potassium sulphate, K_2SO4 and a combination of both types of contaminant. As mentioned earlier, only 12 measurements were performed for each class and the output of the three sensors was gathered for analysis. When 12 measurements for each sensor are made, there will be 36 data sets for each class. The energy and mean of approximation in level 4 and also the energy of details in all levels were calculated.

Fig. 12 illustrates the typical three dimensional inputs of class 1 for the ANN. Based on Fig. 12, the feature of the inputs are shown in three dimensions to represent their graphical state before these input vectors are classified. From Fig. 12, the three classes located inside the blue circle is clearly placed separately in different locations

Table 1 Classes of water sample in each group

	Potassium Nitrate, KNO_3 (ppm)	Potassium Sulphate, K_2SO_4 (ppm)
Class 1	5.0	-
Class 2	10.0	-
Class 3	15.3	-
Class 4	21.2	-
Class 5	60.3	-
Class 6	113.5	-
Class 7	-	5.5
Class 8	-	10.6
Class 9	-	15.0
Class 10	-	20.6
Class 11	-	60.5
Class 12	-	110.0
Class 13	5.0	5.0
Class 14	10.2	10.1
Class 15	15.4	15.3
Class 16	40.3	40.0
Class 17	60.3	60.5
Class 18	80.2	80.4
Class 19	100.4	100.2

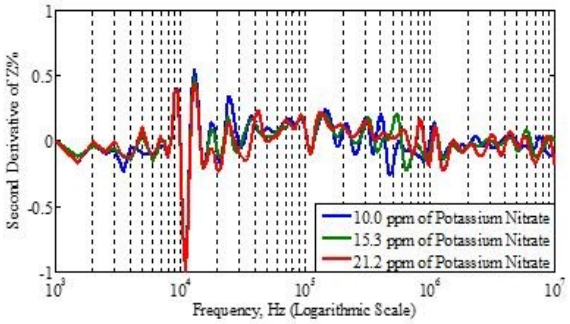

Fig. 9 Second derivative for three potassium nitrate signals

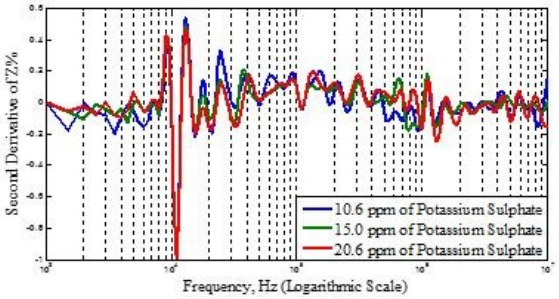

Fig. 10 Second derivative for three potassium sulphate signals

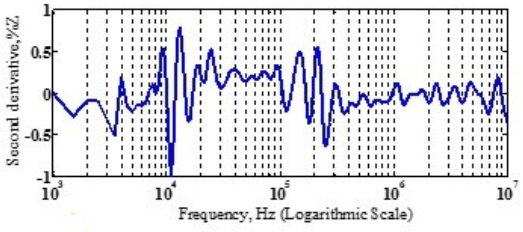

a) Original signal of class 1

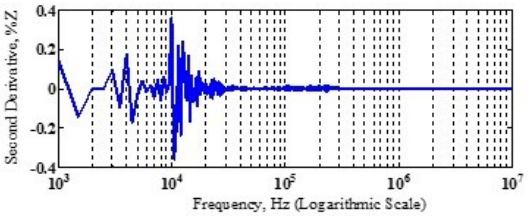

(b) graphs at level 1

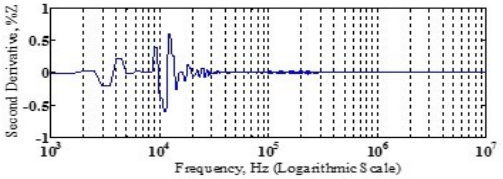

(c) graphs at level 2

Fig. 11 Signal decomposition by Haar wavelet

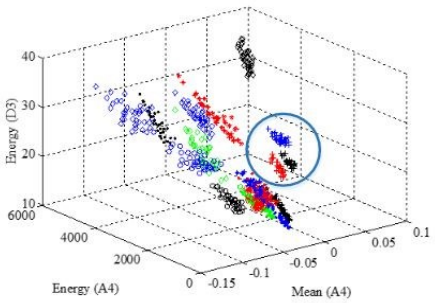

Fig. 12 The three dimensional inputs data of Energy A3, Energy A4 and Mean A4 of class 1

The total size of data is 6×684 where 6 represent the dimension of features while 684 represent the total number of all samples in 19 classes. Each class comprises of 36 samples that have been categorized into three data sets known as train, validation, and test. From a total of 36 samples, 70 % is used for train, 10 % for validation, and 20 % for test.

4.10 Multilayer Perceptron (MLP) Architecture in Neural Network

A typical three layers of MLP as shown in Fig. 13 which consists of inputs, outputs and activation layer. The trial and error method is used to obtain the optimum architecture of three layers MLP. Firstly, a network with six neurons located in hidden layer is used as an initial guess. Sigmoid function and linear function are applied in the hidden layer and the output layer, respectively.

4.11 Input Space for Neural Network

The optimum parameter has to be obtained in order to optimize the performance of the neural network. To achieve the optimal parameter of the neural network, the square mean error of both training and validation sets based on Equation (4) is determined. The trial and error approach is used to determine the number of neuron in the hidden layer. Hence, Fig. 14 shows the plot of error for training the data as the number of neurons in hidden layer changed.

Based on Fig. 14, the error of the training data decreases as the number of neurons in a hidden layer increases in which the number of neurons exceeds 20. Furthermore, when the number of neurons in the hidden layer is more than 20, the error is slightly decreasing. However, the additional neurons in hidden layer caused the compl exity of the network, which caused an increase in the computational time. Therefore, a compromise between network complexity and error reduction is achieved by selecting 25 neurons to be constructed in the hidden layer.

Apart from that, Fig. 14 also illustrates the local minima problem of neural network where the error of training data fluctuated. The local minima caused the system to be looped at a certain point on the data set which lead to a loss of another important data. This error occurred at several points where the number of neurons selected were 14, 16, 25, and 34. The three layers MLP was trained in the local minima (LM) mode where the learning mode is set to be 0.001.The training for the MLP used the mean square error as the objective function where the mean square error was also based on Equation (4). Fig. 15 illustrates the error was reduced during three stages of process, namely, training, validation and testing.

Fig. 15 also shows the best error plot for 61 epochs. Based on that, the iteration at which the validation performance reached minimum was 55 and then the training process continued for another six iterations before the training stopped. From Fig. 15, it also shows that none

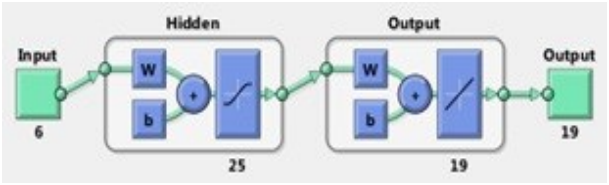

Fig. 13 Structure of Multilayer Perceptron (MLP)

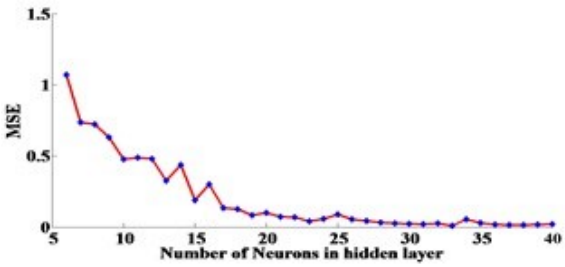

Fig. 14 The error of training data as the number of hidden layer is manipulated

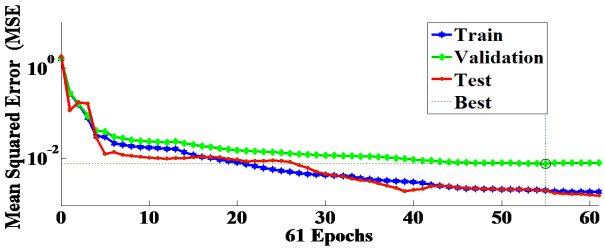

Fig. 15 The error for each stage of training procedure

Table 2: The characteristic performance of the classification method with and without ANN

Descriptions	Result of ANN
Multilayer Perceptron (MLP)	2-25-19
Incorrect training and validation samples (out of 551 samples)	7
Incorrect test samples (out of 133 samples)	2
RMSE for all data sets (%)	0.0132

of the training data is over-fitting. This is due to the test and validation data sets that follow the training error.

The optimum performance of three layer MLP is shown in Table 2. As clearly stated in Table 2, the root mean square error (RMSE) for all data sets is 0.0132. Besides, it could be seen that the number of errors for the incorrect samples was as low as 9 out of 684. This means that, the error is very low and this feature extraction method that consists of mean and energy is suitable for the input layers of the MLP neural network structure.

5. Conclusion

This paper has shown that the innovation from the concept of novel sensor based on the combination of planar meander and interdigital sensors can be used to detect nitrate and sulphate in water sources. Based on the results obtained from the sensor array, the impedance response is directly related with the level of concentration of nitrate and sulphate solutions. The contrasts between the signals obtained from the sensor array can be clearly seen after the signals converted into its respective second derivatives.

Before the ANN can be used as a classification tool, a few criterion such as the proper types and forms of inputs for the ANN, multilayer perceptron parameters of the ANN, and limitations of the ANN need to be considered in constructing the structures of ANN. Hence, the input signals for the ANN need to be reduced using Discontinuous Wavelet Transform (DWT) and Haar wavelet. Then, the approximation and details of mean and energy of the signals are extracted to form the MLP inputs.

A three layers MLP that consists of an input layer, hidden layer, and output layer is trained, validated, and tested in successive steps to classify 19 classes of the nitrate and sulphate water samples. The optimal number of 25 hidden neurons in the network is gained during the training and validation process. The number of hidden neurons is determined based on the calculated minimum square error. Based on the results obtained, the ANN method could estimate the level of nitrate and sulphate concentration with the relative mean square error (RMSE) of 0.0132.

Acknowledgement

The authors would like to acknowledge the financial support from the Science fund grant from the Ministry of Science, Technology and Innovation (MOSTI) Malaysia (Vote No. 03-01-06-SF1216).

References

[1] B. Hull and V. John, *Non-destructive testing*: Springer-Verlag New York Inc.,New York, NY, 1988.

[2] M. B. Mesina, T. P. R. De Jong, and W. L. Dalmijn, "Automatic sorting of scrap metals with a combined electromagnetic and dual energy X-ray transmission sensor," *International Journal of Mineral Processing,* vol. 82, pp. 222-232, Jun 2007.

[3] A. Srinivasan, *Handbook of Precision Agriculture*. New York: The Haworth Press, 2006.

[4] D. Schlicker, A. Washabaugh, I. Shay, and N. Goldfine, "Inductive and capacitive array imaging of buried objects," *Insight,* vol. 48, pp. 302-306, May 2006.

[5] A. R. Mohd Syaifudin, K. P. Jayasundera, and S. C. Mukhopadhyay, "A low cost novel sensing system for detection of dangerous marine biotoxins in seafood," *Sensors and Actuators B: Chemical,* vol. 137, pp. 67-75, 2009.

[6] A. V. Mamishev, K. Sundara-Rajan, F. Yang, Y. Q. Du, and M. Zahn, "Interdigital sensors and transducers," *Proceedings of the 2006 IEEE Sensors Applications Symposium,* vol. 92, pp. 808-845, May 2004.

[7] A. Guadarrama-Santana and A. Garcia-Valenzuela, "Principles and Methodology for the Simultaneous Determination of Thickness and Dielectric Constant of Coatings with Capacitance Measurements," *IEEE Transactions on Instrumentation and Measurement,* vol. 56, pp. 107-112, 2007.

[8] B. George, H. Zangl, T. Bretterklieber, and G. Brasuer, "A Combined Inductive-Capacitive Proximity Sensor and Its Application to Seat Occupancy Sensing," presented at the I2MTC-International Instrumentation and Measurement, Singapore, 2009.

[9] N. Kirchner, D. Hordern, D. K. Liu, and G. Dissanayake, "Capacitive sensor for object ranging and material type identification," *Sensors and Actuators a-Physical,* vol. 148, pp. 96-104, Nov 4 2008.

[10] H. M. Greenhou, "Design of Planar Rectangular Microelectronic Inductors," *IEEE Transactions on Parts Hybrids and Packaging,* vol. 10, pp. 101-109, 1974.

[11] H. Y. Hwang, S. W. Yun, and I. S. Chang, "A design of planar elliptic bandpass filter using SMD type partially metallized rectangular dielectric resonators," *2001 IEEE Mtt-S International Microwave Symposium Digest,* vol. 3, pp. 1483-1486, 2001.

[12] K. Um and B. An, "Design of rectangular printed planar antenna via input impedance for supporting mobile wireless communications," *Proceeedings of IEEE 55th Vehicular Technology Conference, Vtc Spring 2002,* vol. 2, pp. 948-951, 2002.

[13] J. Yunas, N. A. Rahman, L. T. Chai, and B. Y. Majlis, "Study of coreless planar inductor at high operating frequency," *Proceedings of 2004 IEEE International Conference on Semiconductor Electronics,* pp. 606-610, 2004.

[14] J. Fava and M. Ruch, "Design, construction and characterisation of ECT sensors with rectangular planar coils," *Insight,* vol. 46, pp. 268-274, May 2004.

[15] J. L. Quirarte, M. J. M. Silva, and M. S. R. Palacios, "Software for analysis and design of rectangular planar arrays," *2004 1st International Conference on*

Electrical and Electronics Engineering (ICEEE), pp. 90-95, 2004.

[16] D. Valderas, J. Melendez, and I. Sancho, "Some design criteria for UWB planar monopole antennas: Application to a slotted rectangular monopole," *Microwave and Optical Technology Letters,* vol. 46, pp. 6-11, Jul 5 2005.

[17] L. W. Li, Y. N. Li, and J. R. Mosig, "Design of a novel rectangular patch antenna with planar metamaterial patterned substrate," *2008 IEEE International Workshop on Antenna Technology: Small Antennas and Novel Metamaterials - Conference Proceedings,* pp. 119-122, 2008.

[18] H. Oraizi and M. T. Noghani, "Design and Optimization of Linear and Planar slot Arrays on Rectangular Waveguides," in *38th European Microwave Conference, 2008. EuMC 2008*, Amsterdam, 2008, pp. 1468-1471.

[19] J. O. Fava, L. Lanzani, and M. C. Ruch, "Multilayer planar rectangular coils for eddy current testing: Design considerations," *Ndt & E International,* vol. 42, pp. 713-720, Dec 2009.

[20] N. J. Goldfine, "Magnetometers for Improved Materials Characterization in Aerospace Applications," *Materials Evaluation,* vol. 51, pp. 396-405, Mar 1993.

[21] N. J. Goldfine and D. Clark, "Near-surface material property profiling for determination of SCC susceptibility," presented at the in 4th EPRI Balance-of-Plant Heat Exchanger NDE Symp, 1996.

[22] S. Yamada, H. Fujiki, M. Iwahara, S. C. Mukhopadhyay, and F. P. Dawson, "Investigation of printed wiring board testing by using planar coil type ECT probe," *IEEE Transactions on Magnetics,* vol. 33, pp. 3376-3378, Sep 1997.

[23] S. C. Mukhopadhyay, S. Yamada, and M. Iwahara, "Experimental determination of optimum coil pitch for a planar mesh-type micromagnetic sensor," *IEEE Transactions on Magnetics,* vol. 38, pp. 3380-3382, Sep 2002.

[24] S. C. Mukhopadhyay, "Quality inspection of electroplated materials using planar type micro-magnetic sensors with post-processing from neural network model," *IEEE Proceedings-Science Measurement and Technology,* vol. 149, pp. 165-171, Jul 2002.

[25] S.C.Mukhopadhyay,"A novel planar mesh-type microelectromagnetic sensor - Part II: Estimation of system properties," *IEEE Sensors Journal,* vol. 4, pp. 308-312, Jun 2004.

[26] S.C.Mukhopadhyay,"High Performance Planar Electromagnetic Sensors-A Review of Few Applications," in *New Zealand National Conference on Non-Destructive Testing*, 2004, pp. 33-41.

[27] S.C.Mukhopadhyay, "Novel planar electromagnetic sensors: Modeling and performance evaluation," *Sensors,* vol. 5, pp. 546-579, Dec 2005.

[28] Y. Sheiretov, D. Grundy, V. Zilberstein, N. Goldfine, and S. Maley, "MWM-Array Sensors for In Situ Monitoring of High-Temperature Components in Power Plants," *IEEE Sensors Journal,* vol. 9, pp. 1527-1536, Nov 2009.

[29] M. A. M. Yunus and S. C. Mukhopadhyay, "Novel Planar Electromagnetic Sensors for Detection of Nitrates and Contamination in Natural Water Sources," *IEEE Sensors Journal,* vol. 11, pp. 1440-1447, 2011.

[30] K. D. AnimAppiah and S. M. Riad, "Analysis and design of ferrite cores for eddy-current-killed oscillator inductive proximity sensors," *IEEE Transactions on Magnetics,* vol. 33, pp. 2274-2281, May 1997.

[31] D. Karunanayaka, Gooneratne, C. P., Mukhopadhyay, S. C., and Sen Gupta G. , "A Planar Electromagnetic Sensors Aided Non-destructive Testing of Currency Coins," *NDT.net* vol. 11, pp. 1-12, Sept 2006.

[32] K. Sundara-Rajan, L. Byrd, and A. V. Mamishev, "Moisture content estimation in paper pulp using fringing field impedance Spectroscopy," *IEEE Sensors Journal,* vol. 4, pp. 378-383, Jun 2004.

[33] S. M. Radke and E. C. Alocilja, "Design and fabrication of a microimpedance biosensor for bacterial detection," *IEEE Sensors Journal,* vol. 4, pp. 434-440, Aug 2004.

[34] N. Sekiguchi, T. Komeda, H. Funakubo, R. Chabicovsky, J. Nicolics, and G. Stangl, "Microsensor for the measurement of water content in the human skin," *Sensors and Actuators B-Chemical,* vol. 78, pp. 326-330, Aug 30 2001.

[35] P. Furjes, A. Kovacs, C. Ducso, M. Adam, B. Muller, and U. Mescheder, "Porous silicon-based humidity sensor with interdigital electrodes and internal heaters," *Sensors and Actuators B-Chemical,* vol. 95, pp. 140-144, Oct 15 2003.

[36] A. Mohd Syaifudin, S. Mukhopadhyay, and P. Yu, "Modelling and fabrication of optimum structure of novel interdigital sensors for food inspection," *International Journal of Numerical Modelling: Electronic Networks, Devices and Fields,* vol. 25, pp. 64-81, 2012.

[37] S. M. Radke and E. C. Alocilja, "A microfabricated biosensor for detecting foodborne bioterrorism agents," *IEEE Sensors Journal,* vol. 5, pp. 744-750, 2005.

[38] A. R. M. Syaifudin, K. P. Jayasundera, and S. C. Mukhopadhyay, "A low cost novel sensing system for detection of dangerous marine biotoxins in seafood," *Sensors and Actuators B-Chemical,* vol. 137, pp. 67-75, Mar 28 2009.

[39] A. R. M. Syaifudin, M. A. Yunus, S. C. Mukhopadhyay, and K. P.Jayasundera, "A novel planar interdigital sensor for environmental monitoring," in *Sensors, 2009 IEEE*, Christchurch, New Zealand, 2009, pp. 105-110.

[40] S. C. Mukhopadhyay, C. P. Gooneratne, S. Demidenko, and G. S. Gupta, "Low Cost Sensing System for Dairy Products Quality Monitoring," *Proceedings of the IEEE Instrumentation and*

Measurement Technology Conference, 2005. IMTC 2005. , vol. 1, pp. 244-249, May 2005.

[41] S. C. Mukhopadhyay, G. Sen Gupta, J. D. Woolley, and S. N. Demidenko, "Saxophone reed inspection employing planar electromagnetic sensors," *IEEE Transactions on Instrumentation and Measurement,* vol. 56, pp. 2492-2503, Dec 2007.

[42] S. C. Mukhopadhyay and C. P. Gooneratne, "A novel planar-type biosensor for noninvasive meat inspection," *IEEE Sensors Journal,* vol. 7, pp. 1340-1346, Sep-Oct 2007.

[43] S. C. Mukhopadhyay, S. D. Choudhury, T. Allsop, V. Kasturi, and G. E. Norris, "Assessment of pelt quality in leather making using a novel non-invasive sensing approach," *Journal of Biochemical and Biophysical Methods,* vol. 70, pp. 809-815, 2008.

[44] A. I. Zia, A. R. M. Syaifudin, S. C. Mukhopadhyay, I. H. AlBahadly, P. L. Yu, C. P. Gooneratne*, et al.*, "MEMS based impedimetric sensing of phthalates," in *2013 IEEE International Instrumentation and Measurement Technology Conference (I2MTC)*, 2013, pp. 855-860.

[45] M. A. M. Yunus, V. Kasturi, S. C. Mukhopadhyay, and G. Sen Gupta, "Sheep skin property estimation using a low-cost planar sensor," in *IEEE Instrumentation and Measurement Technology Conference 2009, I2MTC '09*, Singapore, 2009, pp. 482-486.

[46] K. G. Ong, C. A. Grimes, C. L. Robbins, and R. S. Singh, "Design and application of a wireless, passive, resonant-circuit environmental monitoring sensor," *Sensors and Actuators a-Physical,* vol. 93, pp. 33-43, Aug 25 2001.

[47] K. G. Ong, J. Wang, R. S. Singh, L. G. Bachas, and C. A. Grimes, "Monitoring of bacteria growth using a wireless, remote query resonant-circuit sensor: application to environmental sensing," *Biosensors & Bioelectronics,* vol. 16, pp. 305-312, Jun 2001.

[48] K. G. Ong, J. S. Bitler, C. A. Grimes, L. G. Puckett, and L. G. Bachas,"Remote query resonant-circuit sensors for monitoring of bacteria growth: Application to food quality control," *Sensors,* vol. 2, pp. 219-232, Jun 2002.

[49] M. C. Hofmann, F. Kensy, J. Buchs, W. Mokwa, and U. Schnakenberg, "Transponder-based sensor for monitoring electrical properties of biological cell solutions," *Journal of Bioscience and Bioengineering,* vol. 100, pp. 172-177, Aug 2005.

[50] E. L. Tan, W. N. Ng, R. Shao, B. D. Pereles, and K. G. Ong, "A wireless, passive sensor for quantifying packaged food quality," *Sensors,* vol. 7, pp. 1747-1756, Sep 2007.

[51] J. B. Ong, Z. P. You, J. Mills-Beale, E. L. Tan, B. D. Pereles, and K. G. Ong, "A Wireless, Passive Embedded Sensor for Real-Time Monitoring of Water Content in Civil Engineering Materials," *IEEE Sensors Journal,* vol. 8, pp. 2053-2058, Nov-Dec 2008.

[52] B. Sharavanan, P. Jung-Rae, M. Tarisha, A. Niwat, A. Alkim, R. Tenneti*, et al.*, "Conformal Passive Sensors for Wireless Structural Health Monitoring," in *Material and devices for smart systems III*, Boston, 2009, pp. 341-348.

[53] E. W. Stanley and et al., "Wireless temperature sensing using temperature-sensitive dielectrics within responding electric fields of open-circuit sensors having no electrical connections," *Measurement Science and Technology,* vol. 21, p. 075201, 2010.

[54] S. E. Woodard, "SansEC sensing technology - A new tool for designing space systems and components," in *Aerospace Conference, 2011 IEEE*, 2011, pp. 1-11.

[55] E. Dickey, O. Varghese, K. Ong, D. Gong, M. Paulose, and C. Grimes, "Room Temperature Ammonia and Humidity Sensing Using Highly Ordered Nanoporous Alumina Films," *Sensors,* vol. 2, pp. 91-110, 2002.

[56] K. V. Oomman and A. G. Craig, "Metal Oxide Nanoarchitectures for Environmental Sensing," *Journal of Nanoscience and Nanotechnology,* vol. 3, pp. 277-293, 2003.

[57] J. Garcia-Canton, A. Merlos, and A. Baldi, "High-Quality Factor Electrolyte Insulator Silicon Capacitor for Wireless Chemical Sensing," *Electron Device Letters, IEEE,* vol. 28, pp. 27-29, 2007.

[58] J. García-Cantón, A. Merlos, and A. Baldi, "A wireless LC chemical sensor based on a high quality factor EIS capacitor," *Sensors and Actuators B: Chemical,* vol. 126, pp. 648-654, 2007.

[59] A. G. Heath, *Water pollution and fish physiology*: CRC press, 1995.

[60] R. J. Woodman and G. F. Watts, "Measurement and application of arterial stiffness in clinical research: focus on new methodologies and diabetes mellitus," *Medical science monitor: international medical journal of experimental and clinical research,* vol. 9, pp. RA81-RA89, 2003.

[61] T. E. Ingram, A. G. Pinder, D. M. Bailey, A. G. Fraser, and P. E. James, "Low-dose sodium nitrite vasodilates hypoxic human pulmonary vasculature by a means that is not dependent on a simultaneous elevation in plasma nitrite," *American Journal of Physiology-Heart and Circulatory Physiology,* vol. 298, p. H331, 2010.

[62] V. E. Nossaman, B. D. Nossaman, and P. J. Kadowitz, "Nitrates and nitrites in the treatment of ischemic cardiac disease," *Cardiology in review,* vol. 18, p. 190, 2010.

[63] L. Knobeloch, B. Salna, A. Hogan, J. Postle, and H. Anderson, "Blue babies and nitrate-contaminated well water," *Environmental Health Perspectives,* vol. 108, p. 675, 2000.

[64] T. Tamme, M. Reinik, and M. Roasto, "Nitrates and nitrites in vegetables: occurrence and health risks," *Bioactive foods in promoting health: fruits and vegetables,* pp. 307-321, 2009.

[65] Ö. Özdestan and A. Üren, "Nitrate and Nitrite Contents of Baby Foods," *Academic Food Journal/Akademik GIDA,* vol. 10, 2012.

[66] D. B. D. Elias, L. B. d. S. Rocha, M. B. Cavalcante, A. M. Pedrosa, I. C. B. Justino, and R. P. Gonçalves, "Correlation of low levels of nitrite and high levels of fetal hemoglobin in patients with sickle cell disease at baseline," *Revista brasileira de hematologia e hemoterapia,* vol. 34, pp. 265-269, 2012.

[67] Y. Sheiretov, D. Grundy, V. Zilberstein, N. Goldfine, and S. Maley, "MWM-array sensors for in situ monitoring of high-temperature components in power plants," *Sensors Journal, IEEE,* vol. 9, pp. 1527-1536, 2009.

[68] N. Goldfine, "Near surface material property profiling for determination of SCC susceptibility," in *4th EPRI Balance-of-Plant Heat Exchanger NDE Symposium, WY, June 10-12, 1996*, 1996.

[69] P. Barge, P. Gay, V. Merlino, and C. Tortia, "Item-level Radio-Frequency IDentification for the traceability of food products: Application on a dairy product," *Journal of Food Engineering,* vol. 125, pp. 119-130, 2014.

[70] J. Vanfleteren, M. Gonzalez, F. Bossuyt, Y.-Y. Hsu, T. Vervust, I. De Wolf*, et al.*, "Printed circuit board technology inspired stretchable circuits," *MRS bulletin,* vol. 37, pp. 254-260, 2012.

[71] M. Norhisam, A. Norrimah, R. Wagiran, R. Sidek, N. Mariun, and H. Wakiwaka, "Consideration of theoretical equation for output voltage of linear displacement sensor using meander coil and pattern guide," *Sensors and Actuators A: Physical,* vol. 147, pp. 470-473, 2008.

[72] H. Wakiwaka, H. Nishizawa, S. Yanase, and O. Maehara, "Analysis of impedance characteristics of meander coil," *Magnetics, IEEE Transactions on,* vol. 32, pp. 4332-4334, 1996.

[73] H. A. Radi and J. O. Rasmussen, "Faraday's Law, Alternating Current, and Maxwell's Equations," in *Principles of Physics*, ed: Springer, 2013, pp. 933-959.

[74] S. Mukhopadhyay, S. D. Choudhury, T. Allsop, V. Kasturi, and G. Norris, "Assessment of pelt quality in leather making using a novel non-invasive sensing approach," *Journal of biochemical and biophysical methods,* vol. 70, pp. 809-815, 2008.

[75] A. I. Zia, M. S. A. Rahman, S. C. Mukhopadhyay, P.-L. Yu, I. Al-Bahadly, C. P. Gooneratne*, et al.*, "Technique for rapid detection of phthalates in water and beverages," *Journal of Food Engineering,* vol. 116, pp. 515-523, 2013.

[76] L. Y. Zhao, "Novel Sensor Design and Application for Detection of Dangerous Contaminated Marine Biotoxins," *Applied Mechanics and Materials,* vol. 416, pp. 980-984, 2013.

[77] S. C. Mukhopadhyay, *Intelligent Sensing, Instrumentation and Measurements* vol. 5: Springer, 2013.

[78] M. A. M. Yunus and S. C. Mukhopadhyay, "Development of planar electromagnetic sensors for measurement and monitoring of environmental parameters," *Measurement Science and Technology,* vol. 22, p. 025107, 2011.

[79] M. A. M. Yunus, S. C. Mukhopadhyay, and S. Ibrahim, "Planar electromagnetic sensor based estimation of nitrate contamination in water sources using independent component analysis," *Sensors Journal, IEEE,* vol. 12, pp. 2024-2034, 2012.

[80] M. A. M. Yunus and S. Mukhopadhyay, "Planar electromagnetic sensor for the detection of nitrate and contamination in natural water sources using electrochemical impedance spectroscopy approach," in *New Developments and Applications in Sensing Technology*, ed: Springer, 2011, pp. 39-63.

[81] M. A. M. Yunus, S. C. Mukhopadhyay, M. S. A. Rahman, N. S. Zahidin, and S. Ibrahim, "The Selection of Novel Planar Electromagnetic Sensors for the Application of Nitrate Contamination Detection," in *Smart Sensors for Real-Time Water Quality Monitoring*, ed: Springer, 2013, pp. 171-195.

[82] M. A. M. Yunus, S. H. Mohamad, A. M. Nor, M. H. Izran, and S. Ibrahim, "Water Content Estimation in Soils Using Novel Planar Electromagnetic Sensor Arrays," *Jurnal Teknologi,* vol. 64, 2013.

[83] A. S. M. Nor, M. A. M. Yunus, S. W. Nawawi, S. Ibrahim, and M. F. Rahmat, "Development of planar electromagnetic sensor array for nitrate and sulphate detection in natural water sources," *Sensor Review,* vol. 35, pp. 106-115, 2015.

[84] M. Faramarzi, M. A. M. Yunus, A. S. M. Nor, and S. Ibrahim, "The application of the Radial Basis Function Neural Network in estimation of nitrate contamination in Manawatu river," in *2014 International Conference on Computational Science and Technology (ICCST)*, Kota Kinabalu, 2014, pp. 1-5.

[85] M. J. Diamantopoulou, D. M. Papamichail, and V. Z. Antonopoulos, "The use of a Neural Network technique for the prediction of water quality parameters," *Operational Research,* vol. 5, pp. 115-125, 2005.

[86] G. Cybenko, "Approximation by superpositions of a sigmoidal function," *Mathematics of control, signals and systems,* vol. 2, pp. 303-314, 1989